

# Optical Engineering

[OpticalEngineering.SPIEDigitalLibrary.org](https://OpticalEngineering.SPIEDigitalLibrary.org)

## Principle demonstration of the phase locking based on the electro-optic modulator for Taiji space gravitational wave detection pathfinder mission

Heshan Liu  
Yuhui Dong  
Ruihong Gao  
Ziren Luo  
Gang Jin

**SPIE.**

Heshan Liu, Yuhui Dong, Ruihong Gao, Ziren Luo, Gang Jin, "Principle demonstration of the phase locking based on the electro-optic modulator for Taiji space gravitational wave detection pathfinder mission," *Opt. Eng.* **57**(5), 054113 (2018), doi: 10.1117/1.OE.57.5.054113.

# Principle demonstration of the phase locking based on the electro-optic modulator for Taiji space gravitational wave detection pathfinder mission

Heshan Liu,<sup>a,†</sup> Yuhui Dong,<sup>b,†</sup> Ruihong Gao,<sup>a,c</sup> Ziren Luo,<sup>a,\*</sup> and Gang Jin<sup>a,c</sup>

<sup>a</sup>Chinese Academy of Sciences, Institute of Mechanics, Beijing, China

<sup>b</sup>Beijing Research Institute of Telemetry, Beijing, China

<sup>c</sup>University of Chinese Academy of Science, School of Engineering Science, Beijing, China

**Abstract.** Weak-light phase locking is a key technology for Taiji space gravitational wave detection and its pathfinder mission. Previously, the phase locking was achieved by a complicated technique, which controls the frequency of the laser via a piezo-electric actuator (kHz range or more) and a temperature actuator (sub-Hz range). We propose an easy phase-locking strategy, which is based on the electro-optic modulator (EOM). Compared with the traditional way, this strategy only needs to modulate the driven voltage of the EOM, and the frequency bandwidth can cover all ranges. An experiment is also established to prove the feasibility of the method. The results show that the noises are  $<80 \mu\text{rad}/\text{Hz}^{1/2}$  in frequencies from 0.2 to 1 Hz, and the thermal drift is the main noise source in our recent system. © 2018 Society of Photo-Optical Instrumentation Engineers (SPIE) [DOI: [10.1117/1.OE.57.5.054113](https://doi.org/10.1117/1.OE.57.5.054113)]

Keywords: Taiji space gravitational wave detection; phase locking; laser interferometer; electro-optic modulator; phasemeter.

Paper 180463 received Mar. 28, 2018; accepted for publication May 10, 2018; published online May 23, 2018.

## 1 Introduction

As a supplement to the observation of an astronomical event by the electromagnetic (EM) radiation, the detection of the gravitational wave (GW) offers an additional tentacle to probe the dark side of our universe, where the EM interaction is weak (perhaps no EM interactions at all), or the EM wave fails to penetrate and reach the earth.<sup>1,2</sup> Similar to the EM radiation, the GW is also a broadband information carrier,<sup>3</sup> the spectrum of which spreads from  $10^{-17}$  Hz to  $>10$  kHz.<sup>3</sup> The ground-based GW detectors, such as LIGO (Laser Interferometer GW Observatory),<sup>4,5</sup> Virgo (Virgo GW observatory),<sup>6</sup> KAGRA/LCGT (Large-scale Cryogenic Gravitational-wave Telescope),<sup>7</sup> IndIGO (Indian Initiative in Gravitational Wave Observations),<sup>8</sup> ET (Einstein Telescope),<sup>9</sup> are sensitive to the medium–high frequency GW signals from deca-Hz to kilo-Hz. However, the GW signals in the medium–low frequencies from milli-Hz to deci-Hz are believed to have much richer astronomical significance. The information carried by such GWs can help us to unveil the evolution of the universe, such as the large-scale structure formation, massive black holes, and galaxies, where the massive black holes are harbored in Ref. 10. To build the medium–low frequency GW detector by means of the laser interferometer, the effective arm length needs to be millions of kilometer. Limited by the earth curvature and seismic noise barrier, the medium–low laser interferometer GW detector has to be built in space.<sup>11,12</sup>

The Laser Interferometer Space Antenna (LISA) is a space mission to observe the GWs between 0.1 mHz and 1 Hz. It is scheduled to be launched into space in 2034 as a European Space Agency L3 mission.<sup>13–16</sup> Its technology

demonstration mission, LISA pathfinder, was launched at the end of 2015, successfully paving the way for LISA by demonstrating the key technologies.<sup>17</sup> Similar to LISA, Chinese space mission—Taiji, the interferometer arm length of which is 3 million km, initiated by the Chinese Academy of Sciences in 2008, plans to be launched in 2033.<sup>18–20</sup> Before the Taiji mission, there is also a pathfinder mission to validate all the key techniques, such as the intersatellites interferometer, the telescope, the beam pointing, the ranging tone, the phase locking, and so on.<sup>20</sup>

The laser power of Taiji should be about 1 or 2 W because of the limitation of its life span. After million kilometer transmission, only a small fraction of the transmitted laser beam can be received by the detector of the remote satellite because of the large beam divergence and the finite aperture (AP) of the telescope. Instead of the simple reflection, a technique called as weak-light phase locking (WLPL) will be introduced into the remote satellite.<sup>21–25</sup> Finally, the high-power slave laser carrying the complete phase information of the transmitting light is sent back to the local satellite. Similar to LISA, the precision of WLPL for Taiji is  $2\pi \times 10^{-6} \text{ rad}/\text{Hz}^{1/2}$ . For Taiji pathfinder, the requirement is set to be  $2\pi \times 10^{-5} \text{ rad}/\text{Hz}^{1/2}$ . Traditionally, the phase locking is always realized by controlling its frequency via piezo-electric and temperature actuators on the slave laser crystal.<sup>22</sup> This strategy is complicated and difficult to implement in an actual test. Electro-optic modulator (EOM) is an optical device, which utilizes the electro-optic effect to modulate a beam of light. The modulation can be imposed on the phase, the frequency, the amplitude, or the polarization of the beam. Therefore, we can modulate the outgoing beam of the laser through the EOM instead of controlling the frequency of the laser. In this paper, we have demonstrated

\*Address all correspondence to: Ziren Luo, E-mail: [luoziren@imech.ac.cn](mailto:luoziren@imech.ac.cn)

†Contributed equally to this work.

the phase locking based on the EOM for Taiji pathfinder in principle.

In Sec. 2, experimental setups and optical layouts are shown in detail. In Sec. 3, the phasemeter and EOMs, which are the key elements of our experiments, are first calibrated. In Sec. 4, the phase-locking experiments are carried out, and the corresponding results are shown for further discussion.

## 2 Experimental Setups

The optical layouts of our experimental setups are shown in Fig. 1. A solid-state laser (wavelength: 1064 nm, linear polarized, and single mode) is used as the light source. The light is divided by a 50/50 beam splitter (BS). One of the beam directly accesses into an acoustic-optical modulator (AOM), while the other beam accesses into the other one after its spread direction is changed by a reflector. When through the AOMs, both beams are frequency shifted, and the first-order Bragg diffracted beams with the maximum power are selected by the APs. The difference between the modulated values by AOMs is the frequency of the heterodyne interferometric signal. After the APs, the two beams are separately split into reflection and transmission by BSs. Through several functional mirrors, the two reflection beams form a Mach-Zehnder (MZ) interferometer as the phase reference, which is enclosed by the red square frame with the mark “1” in Fig. 1. Meanwhile, the two transmission beams are first passed through two EOMs (Thorlabs EO-PM-NR-C2). One of the EOMs simulates the phase noises of the free running laser, while the other is for the phase divergence compensation between the two laser beams. After that, the other MZ interferometer is formed as an error signal in the phase-locking loop, which is enclosed by the purple square frame with the mark “2” in Fig. 1. Unlike the reference interferometer, there are two photodetectors (PDs).  $PD_a$  is for the in-loop, and  $PD_b$  is for the out-of-loop. The phase divergence between the in-loop signal and the reference signal is measured by the phasemeter and then delivered to the proportional integral derivative (PID) controller. According to the phase divergence, the corresponding voltage, applied to EOM, is calculated by the

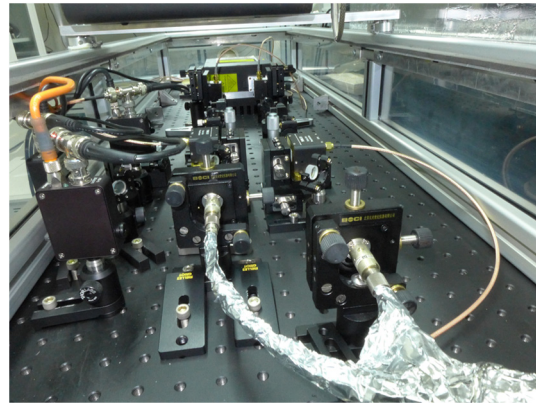


Fig. 2 The physical picture of the phase-locking optical systems.

controller for the phase compensation among the laser beams. The optical system is put on an optical bench enclosed by a cuboid acrylic cage to prevent air convection. The actual physical picture of the optical system is shown in Fig. 2.

## 3 Calibration

### 3.1 Phasemeter Sensitivity

A digital phasemeter with four channels is utilized in our experiment, which is established on a commercial field-programmable gate array platform.<sup>26,27</sup> Prior to the experiment, we have tested the linear property and the noise spectrum of the phasemeter by a functional generator (Agilent 33522A, two channels). In the linear test, two signals (1 MHz) from the generator are, respectively, connected with the first (or arbitrary) two channels of the phasemeter. Phase difference values between the two signals are accurately modulated by the phase modulation of the generator. The degree of the linearity can be obtained by comparing the serial phase values between the setting and the measurement. Noises spectra are tested in the condition of zero measurement, in which the signal of one channel of the generator is divided into four and then this delivers to the channels of the phasemeter,

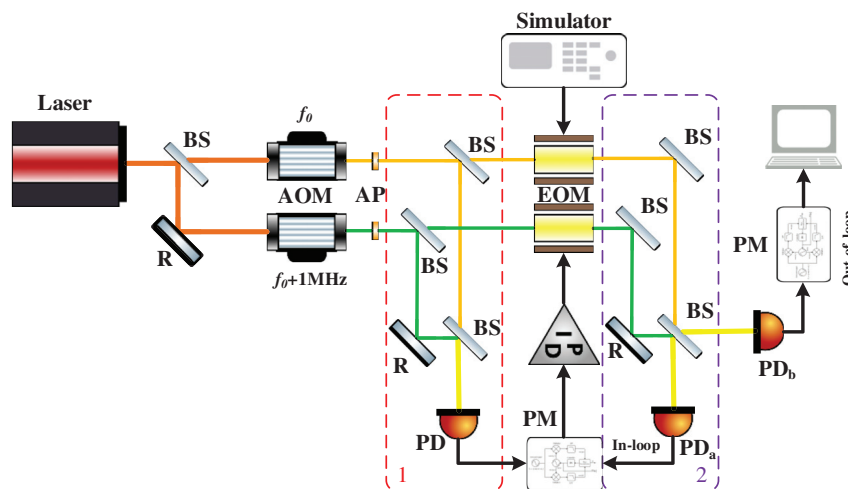


Fig. 1 The optical layout of the experimental systems, and the heterodyne frequency is set to 1 MHz. BS, 50/50 beam splitter; R, reflector; AOM, acoustic-optical modulator; AP, aperture; PM, phasemeter; EOM, electro-optic modulator; PID, proportional integral derivative; and PD, photodetector.

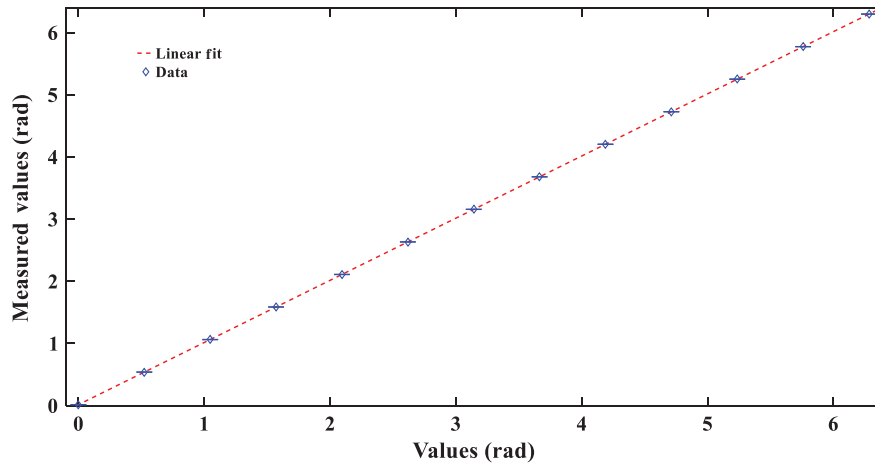


Fig. 3 The linear performance of the phasemeter.

respectively. The results of both experiments are shown in Figs. 3 and 4.

As shown in Fig. 3, the expression of the fit line is  $y = x + 0.0155$ , with the  $R^2$  and the slope equal to 1 (four decimal places). It means that the phasemeter shows an excellent linearity performance. In Fig. 4, the sensitivity of the phasemeter could meet the requirements for Taiji in the frequency ranges of 0.1 to 1 Hz and 0.1 to 1 mHz. However, due to the thermal drift and the sampling jitter, the noise increases largely in the frequencies between 0.1 Hz and 1 mHz. The sampling jitter noise is produced by the sampling jitter of the analog-to-digital converter (ADC). Its value not only relates to the timing jitter of the ADC-driven clock but also the response time jitter of the ADC. By the introduction of the pilot tone,<sup>29</sup> the noise can be suppressed below the Taiji sensitivity curve. The main idea is that the measurement signal is added with a dedicated pilot tone signal (the frequencies of two signals are different). This mixed signal is sampled by the ADC, and the sampling jitter noises of the measurement signal and the pilot tone, which are proportional to each frequency, are recorded by the phasemeter, respectively. Finally, through simple calculations between

the two values, the sampling jitter noise of the measurement signal can be directly removed.

### 3.2 Electro-Optic Modulator Linearity

It is known that the phase modulation  $\phi_m$  depends linearly on the potential  $V_m$  applied to the EOM (Pockels effect,  $\phi_m = A \cdot V_m$ ). Therefore,  $A$  should be calibrated before using. The potential applied to the EOM is linearly increased from 0 to 100 V in 100 s, and the respective phases between the reference and the experimental interferometer are read out by the phasemeter. The calibrated results are shown in Fig. 5.

In Fig. 5, by the linear fit, the expression of the fit line is  $y = 0.01322x$ , and the value of  $R^2$  is equal to 0.9987. It means that modulated phases show a good linearity performance along with the potential increase. So, the translated coefficient of the EOM (the slope of the fit line) is equal to 13.22 mrad/V. The fluctuations around the red line of the phase are mainly due to that the experimental equipment and instruments, such as the optical bench, the radio frequency (RF) coaxial cables, the phasemeter, and the EOMs, are easily influenced by the thermal drift of the

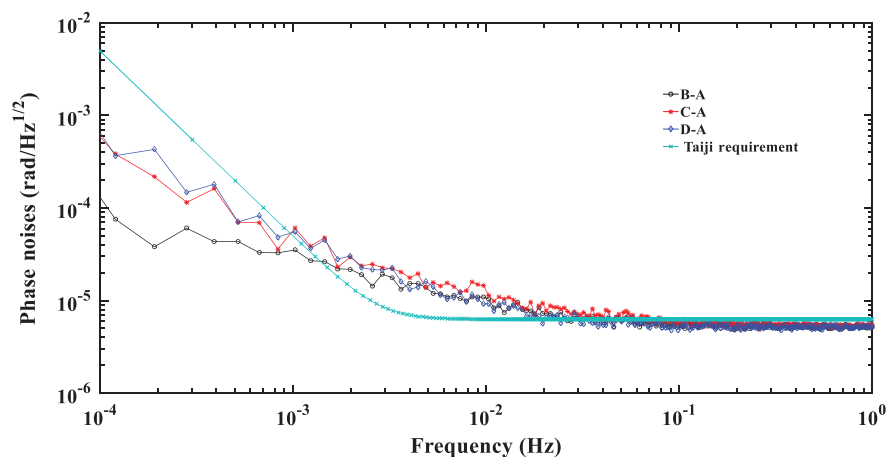
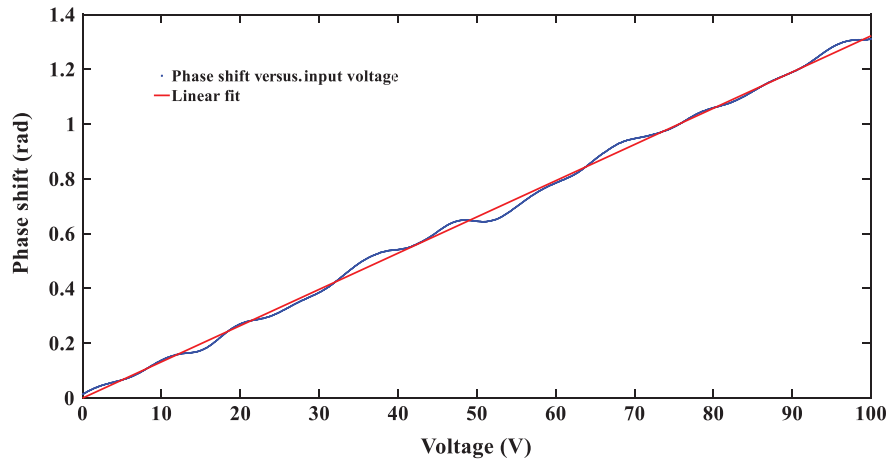


Fig. 4 The typical noises of the phasemeter in the amplitude spectra density. The capitals (A, B, C, and D) represent the respective channels of the phasemeter. The results have been smoothed by the method of linear amplitude spectrum density (LASD),<sup>28</sup> developed by Albert Einstein Institute (Hannover, Germany).



**Fig. 5** The results of the EOM calibrated experiments.

environment, especially when no active temperature control is introduced.

#### 4 Results and Discussions

After the calibrations of the phasemeter and the EOM, the phase-locking experiments are carried out in our lab. The signal from the PD of the reference interferometer is split into two and then connected with channels A and B of the phasemeter for the background noise testing. The signals of the in-loop and the out-of-loop are separately connected with the channels C and D of the phasemeter. Results are shown in Fig. 6.

In Fig. 6, the black line is the background noise of our optical system, in which the common-mode noises are rejected in the ideal condition. The sensitivity can reach  $30 \mu\text{rad}/\text{Hz}^{1/2}$  in the bands of 0.01 to 1 Hz, which are dominated by the electronic noises in our system. Then, the curve slightly increases to  $50 \mu\text{rad}/\text{Hz}^{1/2}$  in the frequencies below 10 mHz, which are influenced by the thermal drift. The pink line is the free running performance of the loop. The largest noise mainly comes from the thermal drift of the environment. The red line is the performance of the in-loop. The value of the red line is the lowest one in Fig. 6 representing

that the PID feedback loop is well working, especially in the lower frequencies bands ( $<0.1$  Hz). The blue line shows the performance of the out-of-loop, which is used to evaluate the noise level of the phase-locking loop. It can be obtained from the line that sensitivity reaches to  $80 \mu\text{rad}/\text{Hz}^{1/2}$  in the frequencies between 0.2 and 1 Hz. Due to the thermal drift, noises increase to  $0.5 \text{ mrad}/\text{Hz}^{1/2}$ , when frequencies decrease to 1 mHz. In addition, a noise obviously locates at 0.2 Hz in every line, except for the black line. The optical system is put on an optical bench enclosed by a cuboid acrylic cage, which has no extra active temperature stabilization control. Moreover, scientific instruments that generate heat, such as the drivers of EOM and laser, the direct current power supplier, the phasemeter, make the temperature field of the optical bench more complex. Therefore, a possible explanation about the noise of 0.2 Hz is that an unknown thermal source from our used instrument or the air conditioner affects the experiment.

Obviously, the thermal drift is the dominant noise source in our optical system. The temperature fluctuation can be coupled into the phase noise directly through many devices, such as the optical bench, the RF coaxial cable, the EOM, the phasemeter, the laser. Moreover, the differential wave-front sensing<sup>30</sup> error and tilt-to-length<sup>31</sup> coupling are aroused by

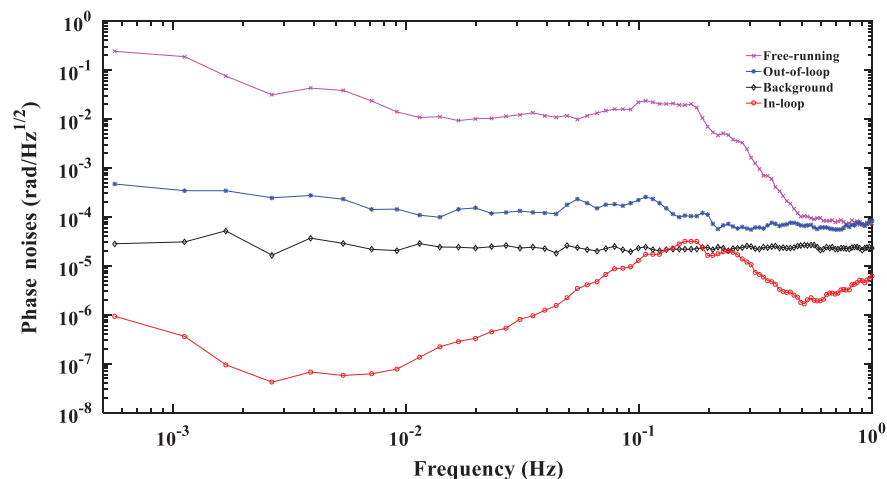


**Fig. 6** The amplitude spectra density of the experiment of phase locking based on EOM, which has also been smoothed by the method of LASD.

the beam angular motion, which is caused by the thermal drift and the environment vibration. In actual fact, the thermal noise is always a combined effect from one or more sources. If we want to decrease the thermal noise to the maximum, any possible heat source should be moved far away from the side of the optical bench, and some effective thermal isolation measures should also be implemented. By the comparison of the results of the free running (pink line) with the out-of-loop (blue line), noises around the whole frequencies band can be well compensated up to 2 orders of magnitude by the phase locking based on EOM, especially in the lower frequencies band ( $<0.1$  Hz). Traditionally, the phase locking is realized by controlling the frequency of the laser via piezo-electric and temperature actuators on the slave laser crystal. The former is used for the feedback loop in kHz range, and the temperature controller is used in sub-Hz range. Differently, the strategy in this paper only needs to modulate the phase of the laser beam through the EOM. The modulation speed of the EOM-driven voltage supplier decides the frequency bandwidth, which includes the kHz and sub-Hz ranges. It means that this strategy can be used as an alternative to replace the traditional phase-locking method in the Taiji pathfinder mission.

## 5 Conclusions and Outlooks

Traditionally, the phase locking was achieved by a complicated technique, which controls the frequency of the laser via a piezo-electric actuator (kHz range or more) and a temperature actuator (sub-Hz range). In this paper, we have successfully established an experiment and proved the feasibility of the phase locking based on the EOM. This strategy only needs to modulate the driven voltage of the EOM, and the frequency bandwidth can cover all ranges. Compared with the traditional way, the phase locking based on the EOM is easy and efficient. The demonstration experiment shows that the noise of the loop is  $<80 \mu\text{rad}/\text{Hz}^{1/2}$  in the frequencies from 0.2 to 1 Hz. Because of the thermal drift, the noise will be increased to  $0.5 \text{ mrad}/\text{Hz}^{1/2}$  in the frequencies below 0.1 Hz. The thermal drift, which can directly couple into phase noises through many devices, is the main noise source in our recent system. To meet the requirement of the Taiji pathfinder, more careful noise analysis of the phase-locking system below 0.1 Hz is needed.

## Acknowledgments

This work was financially supported by the Strategic Priority Research Program of the Chinese Academy of Sciences (Grant No. XDB23030000).

## References

1. D. N. Spergel, "The dark side of cosmology: dark matter and dark energy," *Science* **347**(6226), 1100–1102 (2015).
2. R. D. Blandford, "A century of general relativity: astrophysics and cosmology," *Science* **347**(6226), 1103–1108 (2015).
3. B. S. Sathyaprakash and B. F. Schutz, "Physics, astrophysics and cosmology with gravitational waves," *Living Rev. Relativ.* **12**(2), 1–141 (2009).
4. B. P. Abbott et al., "LIGO: the laser interferometer gravitational-wave observatory," *Rep. Prog. Phys.* **72**(7), 076901 (2009).
5. B. P. Abbott et al., "Observation of gravitational waves from a binary black hole merger," *Phys. Rev. Lett.* **116**(6), 061102 (2016).

6. B. P. Abbott et al., "Prospects for observing and localizing gravitational-wave transients with advanced LIGO and advanced virgo," *Living Rev. Relativ.* **19**(1), 1–39 (2016).
7. R. Kumar et al., "Status of the cryogenic payload system for the KAGRA detector," *J. Phys. Conf. Ser.* **716**, 012017 (2016).
8. C. S. Unnikrishnan, "IndIGO and LIGO-India: scope and plans for gravitational wave research and precision metrology in India," *Int. J. Mod. Phys. D* **22**(01), 1341010 (2013).
9. M. Punturo et al., "The Einstein telescope: a third-generation gravitational wave observatory," *Classical Quantum Gravity* **27**(19), 194002 (2010).
10. P. Binétruy et al., "Cosmological backgrounds of gravitational waves and eLISA/NGO: phase transitions, cosmic strings and other sources," *J. Cosmol. Astropart. Phys.* **2012**(06), 1–72 (2012).
11. J. Gair et al., "Testing general relativity with low-frequency, space-based gravitational-wave detectors," *Living Rev. Relativ.* **16**(7), 1–109 (2013).
12. M. Pitkin et al., "Gravitational wave detection by interferometry (ground and space)," *Living Rev. Relativ.* **14**(5), 1–75 (2011).
13. J. I. Thorpe, "LISA long-arm interferometry," *Classical Quantum Gravity* **27**(8), 084008 (2010).
14. A. Sesana et al., "Space-based detectors," *Gen. Relativ. Gravitation* **46**(12), 1793 (2014).
15. S. Vitale, "Space-borne gravitational wave observatories," *Gen. Relativ. Gravitation* **46**(5), 1730 (2014).
16. M. Armano et al., "The LISA pathfinder mission," *J. Phys. Conf. Ser.* **610**(1), 012005 (2015).
17. M. Armano et al., "Sub-femto-g free fall for space-based gravitational wave observatories: LISA pathfinder results," *Phys. Rev. Lett.* **116**(23), 231101 (2016).
18. X. Gong et al., "A scientific case study of an advanced LISA mission," *Classical Quantum Gravity* **28**(9), 094012 (2011).
19. G. Jin, "Program in space detection of gravitational wave in Chinese Academy of Sciences," *J. Phys. Conf. Ser.* **840**(1), 012009 (2017).
20. W.-R. Hu and Y.-L. Wu, "The Taiji program in space for gravitational wave physics and the nature of gravity," *Natl. Sci. Rev.* **4**(5), 685–686 (2017).
21. S. P. Francis et al., "Weak-light phase tracking with a low cycle slip rate," *Opt. Lett.* **39**(18), 5251 (2014).
22. C. Diekmann et al., "Analog phase lock between two lasers at LISA power levels," *J. Phys. Conf. Ser.* **154**, 012020 (2009).
23. G. J. Dick, M. Strelakov, and K. Birnbaum, "Optimal phase lock at femto-watt power levels for coherent optical deep-space transponder," IPN Progress Report 42-175, Jet Propulsion Laboratory, California (2008).
24. P. W. McNamara, "Weak-light phase locking for LISA," *Classical Quantum Gravity* **22**(10), S243 (2005).
25. Y. Dong et al., "A comprehensive simulation of weak-light phase-locking for space-borne gravitational wave antenna," *Sci. China Technol. Sci.* **59**(5), 730–737 (2016).
26. H. S. Liu et al., "The evaluation of phasemeter prototype performance for the space gravitational waves detection," *Rev. Sci. Instrum.* **85**(2), 024503 (2014).
27. H. S. Liu et al., "Multi-channel phasemeter and its application in the heterodyne laser interferometry," *Sci. China Technol. Sci.* **58**(4), 746–749 (2015).
28. Albert Einstein Institute, "LTPDA," V3.0.13 <https://www.elisascience.org/ltpda/>.
29. O. Gerberding et al., "Phasemeter core for intersatellite laser heterodyne interferometry: modelling, simulations and experiments," *Classical Quantum Gravity* **30**(23), 235029 (2013).
30. Y. H. Dong et al., "Methodological demonstration of laser beam pointing control for space gravitational wave detection missions," *Rev. Sci. Instrum.* **85**(7), 074501 (2014).
31. S. Schuster et al., "Experimental demonstration of reduced tilt-to-length coupling by a two-lens imaging system," *Opt. Express* **24**(10), 10466 (2016).

**Heshan Liu** is a postdoctor at the Institute of Mechanics, Chinese Academy of Sciences. He received his BE degree in engineering mechanics from Harbin University of Science and Technology in 2009, and his PhD in general and fundamental mechanics from the University of Chinese Academy of Sciences in 2015. His current research interests focus on the key technologies of the space gravitational wave detection, such as the laser interferometer, the phase measurement, the laser phase-locking, the laser beam pointing, and so on.

Biographies for the other authors are not available.